

A&A manuscript no.  
(will be inserted by hand later)

Your thesaurus codes are:  
06(08.05.3; 08.09.2  $\eta$  Car; 08.13.2; 09.02.1; 09.10.1)

ASTRONOMY  
AND  
ASTROPHYSICS

December 21, 2000

# High velocity structures in, and the X-ray emission from the LBV nebula around $\eta$ Carinae

K. Weis<sup>1,2,3\*</sup>, W.J. Duschl<sup>1,2</sup>, and D.J. Bomans<sup>4</sup>

<sup>1</sup> Institut für Theoretische Astrophysik, Tiergartenstr. 15, 69121 Heidelberg, Germany

<sup>2</sup> Max-Planck-Institut für Radioastronomie, Auf dem Hügel 69, 53121 Bonn, Germany

<sup>3</sup> University of Illinois, Department of Astronomy, 1002 W. Green Street, Urbana, IL 61801, USA

<sup>4</sup> Astronomisches Institut, Ruhr-Universität Bochum, Universitätsstr. 150, 44780 Bochum, Germany

received; accepted

**Abstract.** The Luminous Blue Variable star  $\eta$  Carinae is one of the most massive stars known. It underwent a giant eruption in 1843 in which the Homunculus nebula was created. ROSAT and ASCA data indicate the existence of a hard and a soft X-ray component which appear to be spatially distinct: a softer diffuse shell of the nebula around  $\eta$  Carinae and a harder point-like source centered on the star  $\eta$  Car. Astonishingly the morphology of the X-ray emission is very different from the optical appearance of the nebula. We present a comparative analysis of optical morphology, the kinematics, and the diffuse soft X-ray structure of the nebula around  $\eta$  Carinae. Our kinematic analysis of the nebula shows extremely high expansion velocities. We find a strong correlation between the X-ray emission and the knots in the nebula and the largest velocities, i.e. the X-ray morphology of the nebula around  $\eta$  Carinae is determined by the interaction between material streaming away from  $\eta$  Car and the ambient medium.

**Key words:** Stars: evolution – Stars: individual:  $\eta$  Carinae – Stars: mass-loss – ISM: bubbles – ISM: jets and outflows

## 1. Introduction

### 1.1. $\eta$ Carinae as a Luminous Blue Variable Star

The star  $\eta$  Carinae, embedded in the large Carina H II complex (the Carina nebula) is still one of the most unique stellar objects in our Galaxy. Known as a variable star for centuries, it brightened up to  $-1^m$  around 1843 (Herschel 1847, Innes 1903, van Genderen & Thé 1984, Viotti

1995, Humphreys et al. 1999) and drastically decreased its brightness by more than  $7^m$  within just 20 years. While the brightness declined, discussions on the nature of this outburst started. A new hint on the origin occurred a century after the burst when nearly simultaneously Gaviola (1946, 1950) and Thackeray (1949, 1950) discovered a nebula around  $\eta$  Car. Since the appearance of the nebula on the first image was of man-like shape, Gaviola named it the *Homunculus*. Today  $\eta$  Car is classified as a *Luminous Blue Variable* (LBV).

The most massive stars (with zero-age main-sequence masses  $\geq 50 M_{\odot}$ ) start as main-sequence O stars and evolve quickly into supergiants. While they cross the Hertzsprung-Russell diagram (HRD) towards the red they seem to enter an unstable phase at an age of roughly  $3 \cdot 10^6$  years (Langer et al. 1994). This phase, the LBV phase, goes along with a very high mass loss (rates up to several  $10^{-4} M_{\odot} \text{ yr}^{-1}$ ). The strong stellar wind and possible giant eruptions where parts of the star's envelope are peeled off, often form circumstellar nebulae, the so called *LBV nebulae* (e.g., Nota et al. 1995). The LBV phase starts when the stars reach the *Humphreys-Davidson limit* (Humphreys & Davidson 1979, 1994) in the HRD. This empirical limit marks the red end of the distribution of very luminous supergiants (Humphreys 1978, 1979 and Humphreys & Davidson 1979). The most luminous, massive stars do not evolve into red supergiants but instead reverse their evolution towards the blue supergiant part in the HRD when they reach the Humphreys-Davidson limit, they turn into LBVs.

With a mass of  $M \sim 120 M_{\odot}$  and a luminosity of  $L \sim 10^{6.7} L_{\odot}$  (Humphreys & Davidson 1994, Davidson & Humphreys 1997)  $\eta$  Car is the most massive member of the LBV class known. In the light of recent discussions about  $\eta$  Car being a binary (Damineli 1996, Damineli et al. 1997, Stahl & Damineli 1998), the masses of the two components would be between 65 and  $70 M_{\odot}$  each. Both components would therefore still be among the most massive stars. The Homunculus nebula is believed to have formed during a giant eruption—the brightness increase

Send offprint requests to: K. Weis, email: [kweis@ita.uni-heidelberg.de](mailto:kweis@ita.uni-heidelberg.de)

\* Visiting Astronomer, Cerro Tololo Inter-American Observatory, National Optical Astronomy Observatories, operated by the Association of Universities for Research in Astronomy, Inc., under contract with the National Science Foundation.

Correspondence to: K. Weis, Institut für Theoretische Astrophysik, Tiergartenstr. 15, 69121 Heidelberg, Germany

of 1843. Images taken with the *Hubble Space Telescope* (HST) revealed the bipolar structure of the Homunculus, consisting of two lobes each about  $8 - 9''$  in diameter (e.g., Morse et al. 1998). The original man-like shape seen around 1950 represents only the brightest emission of the bipolar lobes in the central region. Beside the two lobe structure an equatorial disk was found already through ground-based observations (Duschl et al. 1995). The deepest HST pictures (200s in the F656N-filter) show a larger amount of very complex filamentary structures like knots, arcs and strings (Weis et al. 1999) of which the sizes vary between fractions of arcseconds and several arcseconds. These structures extend much further out than the bipolar Homunculus, up to a distance of at least  $30''$  and form the outer nebula, the so-called *outer ejecta* (Weis 2000, Weis & Duschl, in prep.). The LBV nebula around  $\eta$  Carinae therefore consists of the inner bipolar Homunculus ( $\sim 17''$  in diameters) and the filamentary outer ejecta (up to  $60''$  across).

Kinematic analysis of the nebula around  $\eta$  Carinae detect astonishingly high expansion velocities, especially in the outer ejecta. In several publications radial velocities of the bipolar central and the outer nebula as high as  $1000 \text{ km s}^{-1}$  were reported (Meaburn et al. 1987, 1993, 1996, Hillier & Allen 1992, Weis et al. 1999, Weis & Duschl, in prep.). Similar velocities were derived from proper motion measurements (Walborn 1976, Walborn et al. 1978, Walborn & Blanco 1988, Currie et al. 1996).

$\eta$  Car was also found to emit in the X-ray regime, with the star being an individual point source and the dominant contributor of hard X-rays while an extended soft X-ray emission was observed from the nebula around  $\eta$  Carinae.

### 1.2. Chronology of the X-ray observations

X-ray emission of the  $\eta$  Car complex was detected by Hill (1972), observing with a proportional counter system aboard a *Terrier-Sandhawk* rocket. Observations with *Ariel 5* (Seward et al. 1976), *OSO 8* (Becker et al. 1976, Bunner 1978) and *Uhuru* (Forman et al. 1978) followed. With the launch of the *Einstein Observatory* the resolution of X-ray images was pushed down to a few arcseconds with the high resolution imager (HRI). Therefore for the first time the X-ray sources in the Carina complex could be resolved into several stars and a soft X-ray emitting diffuse component of the larger Carina H II complex (Seward et al. 1979, Seward & Chlebowski 1982).  $\eta$  Car itself was just one extended source. The extended soft X-rays compared to the optical data, showed their origin in the nebula around  $\eta$  Carinae (Seward et al. 1979). The authors excluded a supernova as formation mechanism for the X-radiation and proposed that they formed through a blast wave from the  $\eta$  Car outburst. The Einstein observations also showed that there was a hard X-ray source located somewhere in the Homunculus.

The first detailed analysis of the X-rays from  $\eta$  Car and its nebula, with a longer Einstein observation, as well as a comparison of the X-ray with the optical image was done in 1984 (Chlebowski et al.). This first overlay already identified the most intense X-ray emission with structures in the outer ejecta, namely the *S condensation*, the *W arc* and the *E condensation* (for the notation of the knots see Walborn 1976). The observed X-rays result mainly from the outer shell of  $\eta$  Car and are soft in nature. In addition the harder central source (not resolved with the Einstein *Imaging Proportional Counter*, IPC) was tentatively identified with the star  $\eta$  Car itself. The measurements of the *Ginga* satellite sensitive to hard X-rays ( $2 - 37 \text{ keV}$ ) prove the existence of a harder source with a temperature of  $4.1 \text{ keV}$  in the Carina nebula (Koyama et al. 1990).

ROSAT improved the resolution and sensitivity in the soft X-ray band even further.  $\eta$  Car was observed with ROSAT in both the *Position Sensitive Proportional Counter* (PSPC; spatial resolution  $\sim 25''$ ) and in the *High Resolution Imager* (HRI; spatial resolution  $\sim 5''$ ). Several discussions on the ROSAT data prove now the existence of a harder and softer X-ray component of  $\eta$  Car and its nebula (c.f., Corcoran et al. 1994, 1995, 1996, 1997), which are spatially distinct: a softer diffuse shell of the nebula and a harder point-like source centered on  $\eta$  Car. In addition it was found that the hard X-ray source shows variability and a pointlike character (Corcoran et al. 1995).

Analogous results were achieved with the *Advanced Satellite for Cosmology and Astrophysics* (ASCA; Tsuboi et al. 1997, Corcoran et al. 1998). Due to the good spectral resolution of ASCA it was also possible to conclude that the 'X-ray variability does not involve measureable changes to the spectral shape of the emission' (Corcoran et al. 1998).

### 1.3. Structure of the paper

In this paper, we present the results of a comparative study of images from the HST, high-resolution long-slit echelle spectra and X-ray data. We will give an interpretation of the origin of the X-rays and explain the different morphological appearance of the optical and the X-ray emission of the nebula around  $\eta$  Car.

## 2. Observation and data reduction

### 2.1. X-ray data

For the analysis of the X-ray emission from the LBV nebula around  $\eta$  Car we made use of archived data from the *Röntgensatellit (ROSAT)*. The ROSAT satellite was sensitive to X-ray emission between  $0.1$  and  $2.4 \text{ keV}$ . Images of the  $\eta$  Car region were taken with the PSPC as well as the HRI. We used mainly the high spatial resolution data taken with the HRI (first HRI images published by Corcoran et al. 1996) since the small X-ray nebula around  $\eta$

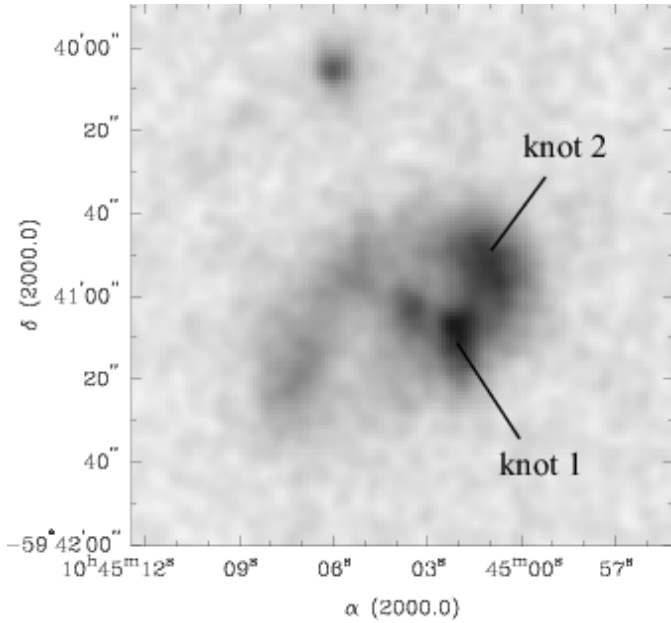


**Fig. 1.** ROSAT HRI image of the full usable integration time of  $\eta$  Car and its nebula. The field of view is about  $2' \times 2'$ . The image was smoothed with a Gaussian filter to an effective resolution of  $5''.5$ . The marked knots 1 and 2 are defined in the text.

Car is barely resolved in the PSPC data (Corcoran et al. 1994). All exposures available for the Carina region (see Tab. 1) were retrieved from the *Max-Planck-Institut für Extraterrestrische Physik* (MPE) ROSAT data center.

Data reduction was performed with IRAF<sup>1</sup>/PROS<sup>2</sup>. Three individual HRI pointings were long enough ( $> 5$  ksec) to contain significant information about the diffuse emission around  $\eta$  Car. First we screened the data for periods with excessively high background. Since highest possible spatial resolution was essential for our work, as next step we checked for errors in the aspect solution, using methods similar to the methods described in Harris et al. (1998). To ensure a stable pointing, we excluded observing time with less than three guide stars present. The total usable integration time adds up to 95 ksec. Next we produced images of the individual observational intervals (OBIs) and re-centered these individual images. Shifts were generally small but not negligible, between  $1''$  and  $4''$ . The count rates in the brightest X-ray point source, which could be used for positional shifts, was unfortunately too low to split the OBIs even more into individual phase bins to investigate residual effects of the spacecraft wobble. We chose a blocking factor of 2, resulting in  $1''$  per pixel and smoothed the images slightly with a

<sup>1</sup> IRAF is distributed by the National Optical Astronomy Observatories which is operated by AURA, Inc. under cooperative agreement with the NSF.

<sup>2</sup> PROS is developed, distributed, and maintained by the Smithsonian Astrophysical Observatory, under partial support from NASA contracts NAS5-30934 and NAS8-30751.

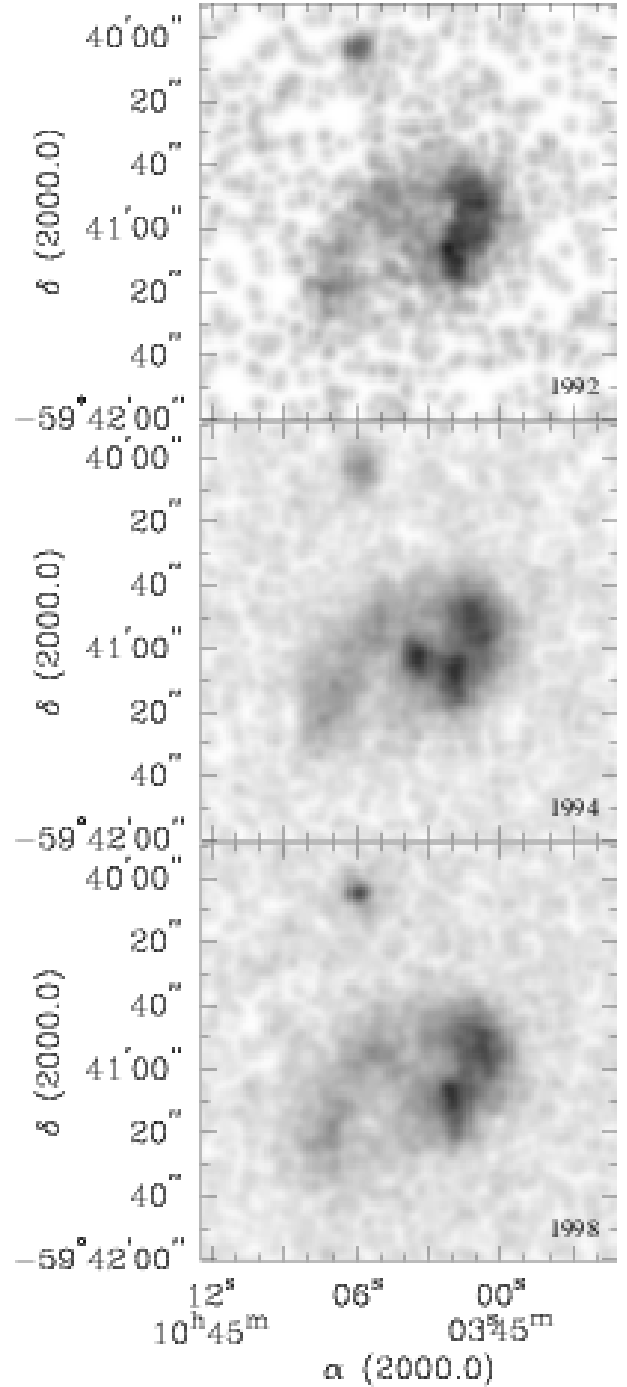


**Fig. 2.** HRI images of the  $\eta$  Carinae nebula during the three observing intervals which are long enough to show the X-ray nebula (see table 1). The three panels show the images generated from the 1992 (upper panel), 1994 (middle panel) 1998 (lower panel) data sets.

$\sigma = 1.5$  pixel Gauss filter. We updated the coordinates using the five X-ray point sources coinciding with the stars HD 93205, HDE303308, CD-59°2635, CD-59°2636, and CD-59°2641 in the Carina nebula. The coordinates of the stars were measured on a Digital Sky Survey (DSS) image using the IRAF/GASP package. The resulting positional

**Table 1.** ROSAT HRI Observations of  $\eta$  Car; the column offset gives the offset of the image center from  $\eta$  Carinae.

pointing	Obs. interval	P.I.	exposure time [s]	offset [']	comment
rh150037n00	900727-900729	Puls	3351	7.135	
rh900385n00	920731-920802	Schmitt	11527	0.31	source off
rh900385a01	940106-940106	Schmitt	522	0.31	
rh900385a02	940721-940729	Schmitt	40555	0.31	source on
rh900644n00	960813-960813	Corcoran	1720	0.31	
rh202331n00	971223-980210	Corcoran	47095	0.31	source off

accuracy of the X-ray images is of the order of  $0''.5$  relative to these stars. From the new photon file we produced three images of the three observations in 1992, 1994 and 1998, according to the central source's high or low state. In addition a total flux image (Fig. 1) was made, combining all observations regardless of the state of the central source. The images are shown in Fig. 2, in which the upper panel gives the 1992 (low state), the middle one the 1994 (high state), and the lower one the 1998 (low state) data.

## 2.2. Optical Imaging

To compare the X-ray data with an optical image of the nebula around  $\eta$  Car, data were taken from the HST Archive at the *Canadian Astronomy Data Centre* (CADC). Images of the *Wide Field Planetary Camera 2* (WFPC2) with the F656N ( $H_\alpha$ ) filter were retrieved<sup>3</sup>. Their reduction, combination and cosmic-ray cleaning followed the standard procedures recommended for WFPC2 data in IRAF. The exposure times ranged from 0.11 to 200 seconds. The reduced and mosaiced F656N image was used for an overlay with the total integration time X-ray image (Fig. 3) and the comparison between the X-ray and the optical emission. In addition it was used to identify several knots in the outer nebula, for which we took kinematic data.

## 2.3. Long-slit echelle spectroscopy

Kinematic information was obtained using long-slit echelle spectroscopy. The data were taken by one of us (KW) with the 4 m Blanco telescope at the *Cerro Tololo Inter-American Observatory* (CTIO) in the long-slit mode. Wavelength selection was achieved by inserting a post-slit  $H_\alpha$  filter (6563/75 Å) and replacing the cross-disperser by a flat mirror. We choose the 79  $\text{mm}^{-1}$  echelle grating, a slit-width of 250  $\mu\text{m}$  ( $\cong 1''.64$ ), which leads to an instrumental FWHM at the  $H_\alpha$  line of about  $14 \text{ km s}^{-1}$ . The data were recorded with the long focus red camera and the Tek2K4 CCD ( $2048 \times 2048$ ). Here the pixel size was  $0.08 \text{ Å pixel}^{-1}$  along the dispersion, and  $0''.26 \text{ pixel}^{-1}$  on the spatial axis. Vignetting limited the slit length to  $\sim 4'$ . During all observations the weather was not photometric

and the seeing was between  $1''.5 - 2''$ . Thorium-Argon comparison lamp frames were taken for wavelength calibration and geometric distortion correction.

The whole dataset contains 31 slit positions, of which the central 6 positions around  $\eta$  Car could not be used, because strong straylight from the dusty Homunculus and extended ghost images did not allow us to extract reliable information from the spectra. The individual observations were offset by  $2''$  each from an offset star rather than  $\eta$  Car itself, since the position of  $\eta$  Car is confused by strong emission of the Homunculus. The orientation and position of the slits are indicated in Fig. 4. With the mapping a field of about  $60'' \times 60''$  around  $\eta$  Car was covered. In Fig. 5 we give three example spectra with individual knots marked by numbers. The spectra cover a range of 80 Å centered on  $H_\alpha$ , thus they include also the [N II] lines at 6548 and 6583 Å. The spatial extent is  $1'.5$ . Usually the features are more prominent in the [N II] lines than in  $H_\alpha$  due to the CNO cycle processed material in the nebula.

Figure 3 shows the overlay of the X-ray emission in contours onto the HST image, velocities (in  $\text{km s}^{-1}$ ) represent the kinematics in the lower panel. Clearly a lack of data can be seen in the center, where the information of the 6 slit positions is missing. A rotation of the slit placed the spectra to a position angle of  $\text{PA} = 132^\circ$ , i.e. along the major axis of the bipolar nebula. A more detailed description of the observations and the spectra will be published separately (Weis & Duschl 2000, in preparation).

## 3. X-rays from the $\eta$ Car region

### 3.1. The morphology of the $\eta$ Car X-ray nebula from ROSAT HRI data

In this paper we concentrate on the X-ray emission from the  $\eta$  Car LBV nebula. The X-ray image with the highest spatial resolution, the ROSAT HRI image, can be seen in Fig. 1.

The X-ray nebula around  $\eta$  Car extends much further out from  $\eta$  Car than the two lobes of the Homunculus (Fig. 3), the *S Ridge* and the *N Condensation* (for notations see Walborn 1976). Instead of the bipolarity of the optical structure, the X-ray nebula consists of a hook-shaped diffuse emission region, roughly encircling the central point-like source. About one-third (position angles  $\text{PA} \approx 210 - 330^\circ$ ) of the loop is of high X-ray surface

<sup>3</sup> F656N – program number: 5239; P.I.: J.A. Westphal; dataset names: U2DH0101T ... U2DH0106T